Are the Badlands of Tapi Basin in Deccan Trap Region of India "Vanishing Landscape?" Badland Dynamics: Past, Present and Future!

10

Veena Joshi and Shreeya Kulkarni

Abstract

Soil erosion is one of the most serious hazards human race is facing today. Four million hectares of agricultural lands have been rendered wastelands in India due to rill and gully erosion. Deccan Trap Region of India is characterized by rocky terrain. Sediments are thin and occupy only restricted areas. The study area is a watershed along the Tapi Basin in Maharashtra where alluvial bank deposits are deeply dissected by intricate network of gullies to form badlands. These badlands have been intensively reclaimed for agriculture in the past few decades. Based on various sedimentological and morphological properties, added by rainfall impact analysis, an assessment has been done to evaluate whether such types of land reclamation practices are permanent solution to the problem of land availability and agriculture in these areas. DEMs of three time periods were self-generated using IRS Cartosat I images and changes in the morphometric parameters were detected from them. A field survey was carried out to measure the current gully reactivation in the area. Results indicate that the region is already indicating soil loss beyond the tolerance limit. A land use planning needs to be designed for these areas because the present land use methods are doing more harm than good.

10.1 Introduction

Soil erosion is said to occur when the external forces exerted by the agents of erosion exceed the resistance provided by the soil surface on which they act. Gullying and land degradation has been a major research in the field of geomorphology for several years. The problem related to this aspect is investigated in many parts of India. Due to the growing population, there is increasing pressure on every patch of land and they have been brought under various land use practices, especially agriculture. This has led to reclamation of all available land, even those which were earlier unfavourable land for cultivation. Badlands are such type of landscape which are often under the pressure of land reclamation now, wherever they are accessible. Badlands are the areas which are rugged, where vegetation is almost absent and are intensely

V. Joshi (✉) · S. Kulkarni
Department of Geography, Savitribai Phule Pune University, Pune, Maharashtra 411007, India
e-mail: veenaujoshi@gmail.com

dissected. They are mostly fluvial in origin characterized by v-shaped valleys, high drainage densities and short steep slopes, often fingered by gently sloping planar surfaces referred to as pediments (Bryan and Jones 1997).

Land degradation in general and soil erosion in particular are the major concerns of the world today. India has an agrarian economy with vast growing population. Soil degradation directly affects agricultural productivity. The intensity of human interference has increased manifold in the last few decades. Better irrigation facilities and new incentives in agriculture in various parts of India, especially Maharashtra also has triggered this factor. Badlands are dynamic and sensitive landscape and previous studies have shown that disturbing them can induce the land to go into positive feedback mechanism and trigger soil erosion (Joshi and Nagare 2009). There are innumerable research works done on the effects of human interference and change in the land-form processes. It is beyond the scope of this paper to include all such studies, however a few classic papers and frequently cited ones and also the studies that are relevant to the present context have been reviewed in the following paragraphs.

The initiation of gullies was the result of unwise utilization of land has been the findings of the study by Wells and Andriamihaja (1993). Removing the natural vegetation has a serious impact on runoff and erosion has been demonstrated by Piegay et al. (2004) and Canton et al. (2004). In India, the study of land cover classification using IRS LISS III image and DEM to understand rugged terrain in Himalayas was carried out by Saha et al. (2005). Gallart et al. (2012) demonstrated high rates of erosion following the reclamation of the badland gullies. Effects of tillage on soil degradation, quality and sustainability were established by Lal in 1993. The physicochemical analysis of clay samples reveals that if organic matter contents can be increased to values above 2%, then remodelled fields tend to stabilize. As a result, some badlands are being irreversibly destroyed and would be better classified as vanishing (Phillips 1998a). The rate of decline of ESP following the reclamation of badlands needs to be ascertained and a

mechanism to link the organic matter content and the ESP needs to be established (Phillips 1998b). The undulating surfaces created after reclamation are likely to result in high rates of erosion in the period immediately following reclamation. This results in an active environment, onto which badlands tend to be re-established. Such badlands have been termed as "strained" as opposed to "vanishing" landscape (Rossi and Vos 1993). The role of organic matter in stabilizing and reducing the erosion of dispersive soils has received less attention than that of non-dispersive soils, although a number of such studies do exist, such as, Dong et al. (1983); Gupta et al. (1984) and Muneer and Oades (1989). A historical approach was adopted by Marathianou et al. (2000) to evaluate land use evolution and degradation in Lesvos (Greece). Reynolds and Stafford (2002) edited a volume on global desertification, questioning the role of humans in causing deserts. Zhang et al. (2007) investigated Land use changes and land degradation in China from 1991 to 2001. A Mediterranean case study of the impact of land use/land cover changes on land degradation dynamics was conducted by Bajocco et al. (2012). Matano et al. (2015) investigated the effects of land use change on land degradation and soil properties along Mara River Basin in Kenya, Tanzania. Land degradation and the sustainability of agricultural production in Nigeria was reviewed by Ajayi (2015). Multivariate analysis was employed by Khaledian et al. (2016) to assess and monitor soil degradation during land use change. Badlands forest restoration was designed in Central Spain by Mongil-Manso et al. in 2016. A scientific conceptual framework was made for land degradation neutrality and to bring land in balance by Cowie et al. (2018). Using Earth observations data, Abdel-Kader (2018) assessed and monitored land degradation in the northwest coast region of Egypt. Batunacun et al. (2019) identified the factors driving land degradation in Xilingol, China. Hazbavi et al. (2019) conducted dynamic analysis of watershed-health based on soil erosion. A bibliometric analysis on land degradation that includes the current scenario, development and future directions was proposed

by Hualin et al. (2020). Land Degradation Neutrality (LDN) indicators were employed to study land use changes in the subalpine forest ecosystems of Korea by Sangsub et al. (2020).

10.2   Study Area

The site for the proposed work is a part of badlands of the Tapi River in the Jalgaon District of Maharashtra in India. It extends approximately between 75° 32′ 3″ E to 75° 33′ 05″ E and 21° 08′ 33″ N to 21° 09′ 10″ N (Fig. 10.1). The average annual rainfall of the area ranges between 630 and 750 mm. The banks along this stretch of the Tapi River are subject to the processes of gullying and ravination, which have transformed a major part of the landscape into badland terrain. There are many pockets along the river banks where deeply dissected badlands are formed. Land reclamation for the purpose of agriculture of these badlands became a very common activity in the whole region now. Some of these watersheds have been completely altered in the last twenty years including the parts of badlands near the Tapi River.

Figure 10.2 depicts the undisturbed parts of the Tapi Badlands, as well as, freshly activated gullies in a field, which was taken in 2013. Figure 10.3 displays the same spot in 2017, where it is seen that all those previous active gullies were filled up and brought under cultivation.

Careful observation of the field revealed that many erosion concentration points have got generated on the cultivated field. It also appeared that those concentration points more or less followed the previous gully network. Google Earth images of different time periods depicting stages of the reclamation of the badlands followed by series of reactivation of the gully network and refilling, a cyclic pattern of land reclamation and gully reactivation have been depicted in Fig. 10.4. It is clear indication that the field has become completely vulnerable now. This field is just one such example in the whole watershed where the same scenario is occurring everywhere. This had led to the formulation of the research objective, whether the current land use practice is a feasible option which would provide a permanent solution to agriculture in the area under review or otherwise.

10.3   Material and Method

In order to achieve the outlined objective, the following methodologies have been adopted in the study.

- Google Earth images from 2006 till present were obtained for observation. The images were examined to understand the phases of the past gully fillings and reactivation history of the field.
- In order to detect the changes in the morphometry resulting from excessive periodic land reclamation, DEMs of three time periods, such as, 2005, 2010 and 2015 were self-generated from IRS (Indian Remote Sensing) Cartosat I stereo images. Leica Photogrammetry suit (Version 9.2) and Arc GIS 10 were used to create the three DEMs. To study the micro-relief of the field, a detailed survey was conducted using dGPS (differential Global Positioning System) to create DEM of the present field morphology at 5 cm resolution.
- Twenty-five sediment samples were collected from the field to study the sediment properties of the area and to evaluate erodibility of these badland sediments. Textural analysis as well as few chemical parameters that have direct relevance with soil erodibility, such as, pH (power of hydrogen), EC (Electric Conductivity), OC (Organic Carbon/ Content), Na (Sodium), K (Potassium), Ca (Calcium), Mg (Magnesium) were detected from the soil samples. Scour depths of 12 samples were calculated from the silt factors to determine the susceptibility of the topsoil under erosion.
- Morphometric parameters were obtained from the Carto DEMs and indices were calculated that have meaningful relations with the present objective of the study.
- Return periods of the rainfall for 500 years were estimated from 60 years rainfall data of the area, using Anderson–Darling goodness-of-fit test and incorporated in the final synthesis.
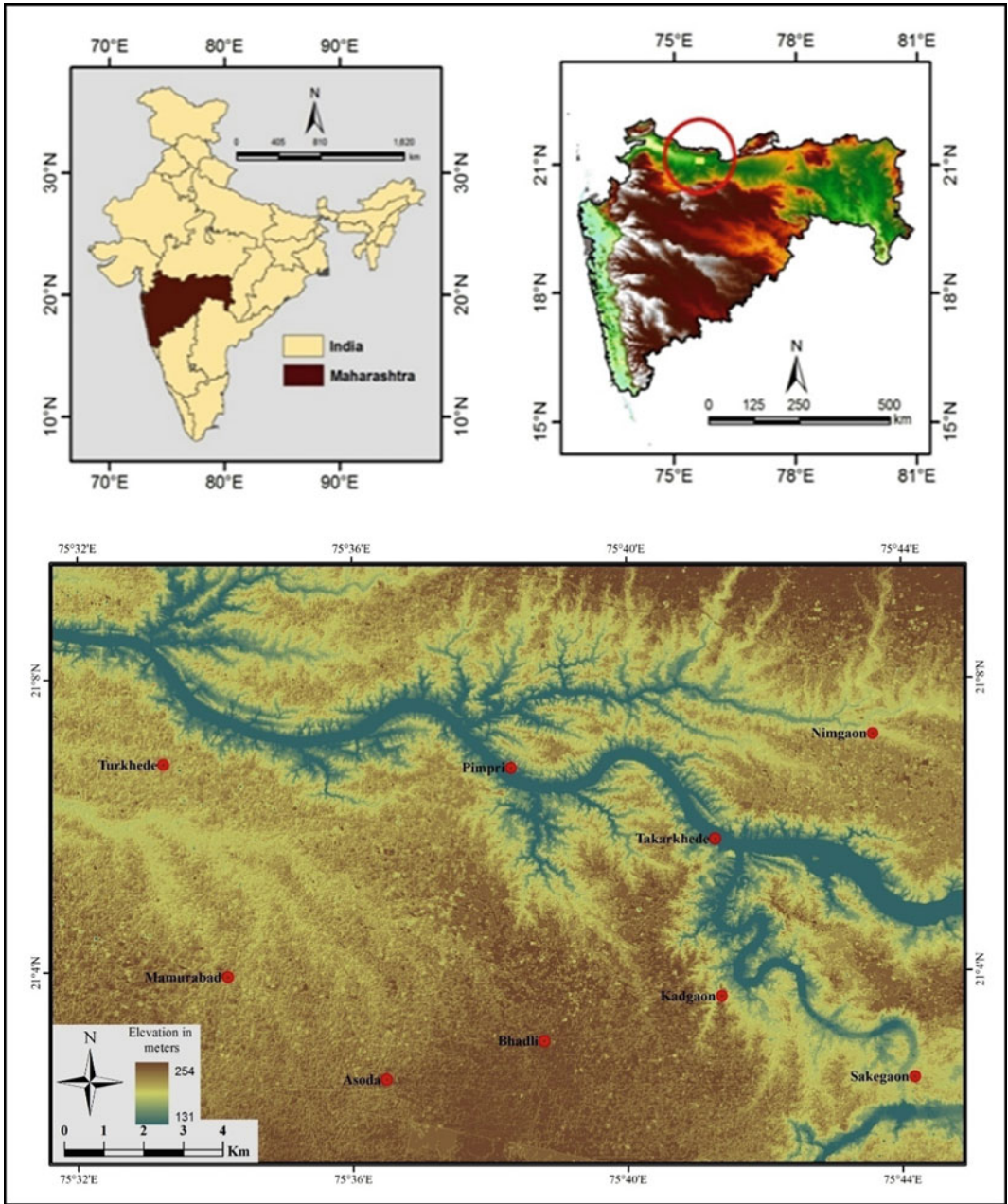
Fig. 10.1 Location map of the study area within Maharashtra state, also showing the DEM of the AOI

Fig. 10.2 The field pictures of the undisturbed parts of the badlands and gully erosion after the clearance of the vegetation and levelling the land for agriculture, within the same watershed

10.4   Results

10.4.1   Comparison of the DEMs

Under the natural conditions, major changes in the hillslope morphology within a time span of 10 years are not expected. But such changes can be possible in an area that is actively interfered by human activities, as in the present study area. Figure 10.5 depicts the flowchart showing the methodology to generate DEM from IRS Cartosat I images and Fig. 10.6 displays the DEMs of the three time periods created at 10 m resolution. The three DEMs were used to assess the changes in the hillslope morphology from 2005 to 2010 and 2015. All the 3 DEMs (12 Dec 2005, 12 Dec 2010, and 10 May 2015) show noteworthy differences in the elevation as well as in the slope.

Remarkable variations can be seen in the relief maps especially between 2005 and 2010

(Fig. 10.7). Relief category between 188 and 254 m increased in the area by 8% between 2005 and 2010. Category between 162 and 177 m decreased by 7% between 2010 and 2015. Changes are more prominent between 2005 and 2010.

Slope of the area also revealed noticeable changes. Area under 14°–29° category increased significantly (5% in five years) from 2005 to 2010 (Fig. 10.8). Area under 14°–29° and 29°–43° categories also increased noticeably (10%, in five years) from 2010 to 2015. Category 0°–14° decreased in the area by 10%. Slope category 43°–57° was absent from 2005 and 2010 DEMs but they start appearing in 2015 DEM. Overall assessment of the slope is that they are visibly changing.

There are a lot of changes in the aspect map also as can be seen in Fig. 10.9. Slope orientation has considerably modified from 2005 to 2010 but the change is not significant between 2010 and 2015. These categories were chosen based on the observation of the main slope aspects of the badland

Fig. 10.3 Scenarios after the badland reclamation are evident in these field pictures. Filling the gullies for cultivation, followed by reactivation of the gully network has been captured in the pictures

terrain in the area. Significant changes in the area can be observed in all the categories. Maximum change can be observed in the category of 71–143 with 15% increase in the area between 2005 and 2010. Category 145–216 and 216–283 decreased by 5% each in the area in the same time. Though the change is slight, pattern remained more or less the same between 2010 and 2015. All the three parameters indicate remarkable changes between 2005 and 2010, implying a major remodelling during this time. Such dramatic changes within such a short time can validate the significant impact of human interference in the region.

Currently, gullies have been filled up and the fields are levelled and put under farming, mainly by cotton and banana. A detailed field observation of the area under review revealed several erosion concentration points and two distinctly activated gullies all across the field.

One of the newly activated gullies oriented towards the main river and another was slopping towards a tributary stream which is situated on one side of the field, guided by an embankment constructed by farmers to reduce erosion of soil from the field. Flutes and pipes were also observed in the field and on the wall of the exposed gullies. In order to conduct a high-resolution mapping of the field, a dGPS survey was conducted for the field and a DEM was created with 5 cm resolution and demonstrated in Fig. 10.10. Erosion concentration points are documented on the DEM. Reactivation of gullies has already began following the path of the old buried gullies, because the energy of the system has not been channelized. These erosion concentration points are targeting the old gully systems because the whole network is controlled by Tapi River. This is a "Downstream controlled" system.
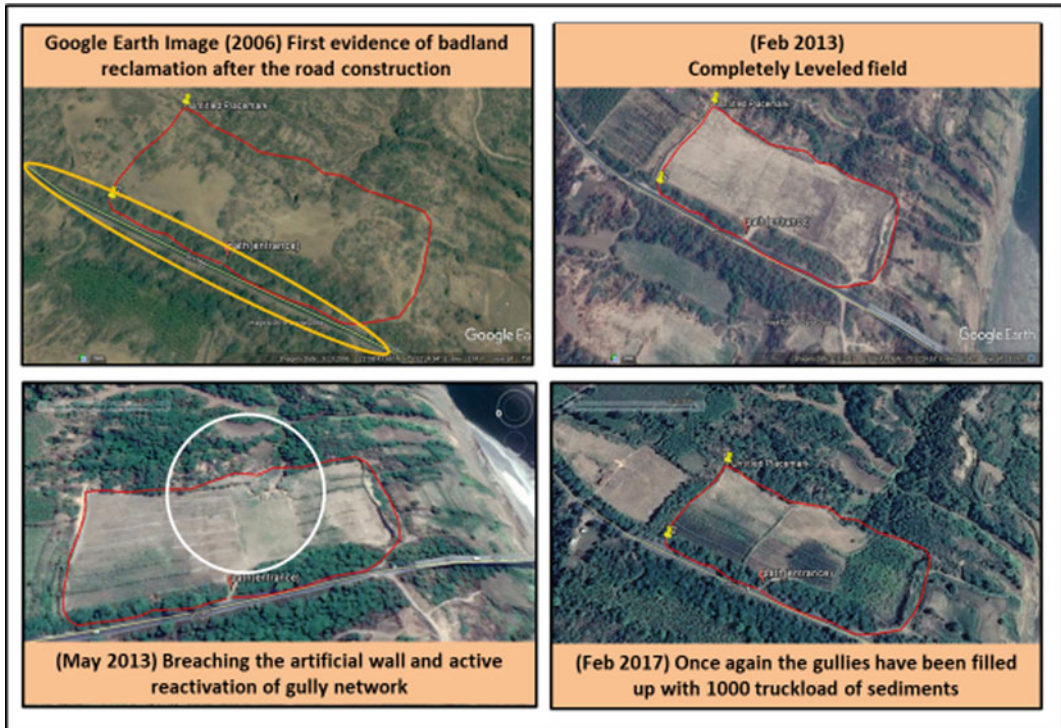
Fig. 10.4 Google Earth images from 2006 till 2016, depicting stages of badland reclamation and gully reactivation in the area (**a** Yellow polygon depicts a road being constructed making the badland watersheds accessible. The reclaimed field is right across the head of an active tributary gully of Tapi River, **b** increase in the reclaimed areas, **c** reactivation of the previous gully after a heavy storm and **d** refilling of the gullies)

10.4.2 Sediment Analysis

Sediments play a crucial role in determining the vulnerability of a region under erosion. Certain sediment properties are known to have a direct influence in the erodibility and a few of such relevant parameters have been detected and the results are presented in the following sections.

10.4.2.1 Power of Hydrogen (pH)

Soil pH is determined by the concentration of hydrogen ions (H^+). It is a measure of the acidity and alkalinity of a soil solution on a scale from 0 to 14. Common acid-forming cations are hydrogen (H^+), aluminium (Al^{3+}) and iron (Fe^{2+} or Fe^{3+}), whereas common base-forming cations include calcium (Ca^{2+}), magnesium (Mg^{2+}), potassium (K^+) and sodium (Na^+) (McCauley et al. 2017). Figure 10.11 demonstrates general pH chart provided by McCauley et al. (2017) and the detected pH values of the sediment samples from the field. pH values range from 7 to 10. Samples ranging between 8 and 10 are sodic in nature McMauley et al. (2017). Following this criterion, the samples are showing a general trend towards sodicity.

10.4.2.2 Organic Matter Content

Organic matter influences the aggregate stability of the soil. Erodible soils contain less than 3.5% of organic matter. Clay particles combine with organic matter form soil aggregates which are usually resistant to erosion. Soil erodibility (K factor) is lessened by larger structural aggregates and rapid soil permeability (Morgan, 1986). The percent organic matter contents of the samples from the field was tested in Zuare Agro, Pune. Figure 10.12 indicates the results of organic content and it reveals that 2/3rd of the samples contain less than 2%. A threshold of 2% is

Fig. 10.5 Flow chart demonstrating steps of the generation of DEM from Cartosat I images, in Leica Photogrammetry Suit 9.2 and Arc GIS 10
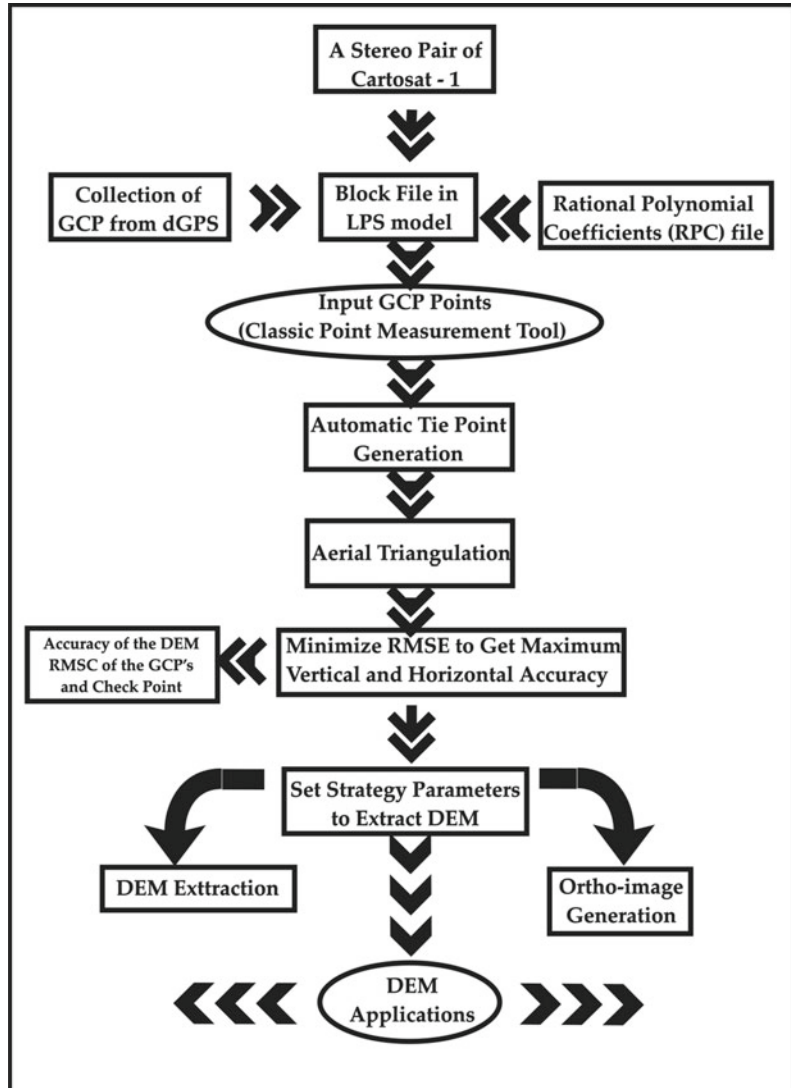
generally accepted for the aggregate stability of the soils.

10.4.2.3 Electrical Conductivity

Soil electrical conductivity (EC) is a measure of the amount of salts in soil (salinity of soil). It is an important indicator of soil-health. EC is correlated to the concentrations of nitrates, potassium, sodium, chloride, sulfate and ammonia but does not provide a direct measurement of salt compounds. Electric conductivity of the samples appears to follow a trend towards changes in textural composition and the topographical

position they occupy. EC for the present samples shows great variability and not systematically related to the depth from which the samples were collected. The values of range from 0.16–0.71 mmho/cm. (Fig. 10.12). There is an inverse relationship between EC and soil erodibility. Keeping all other factors constant, if EC is low the rate of removal of soil is low and vice versa.
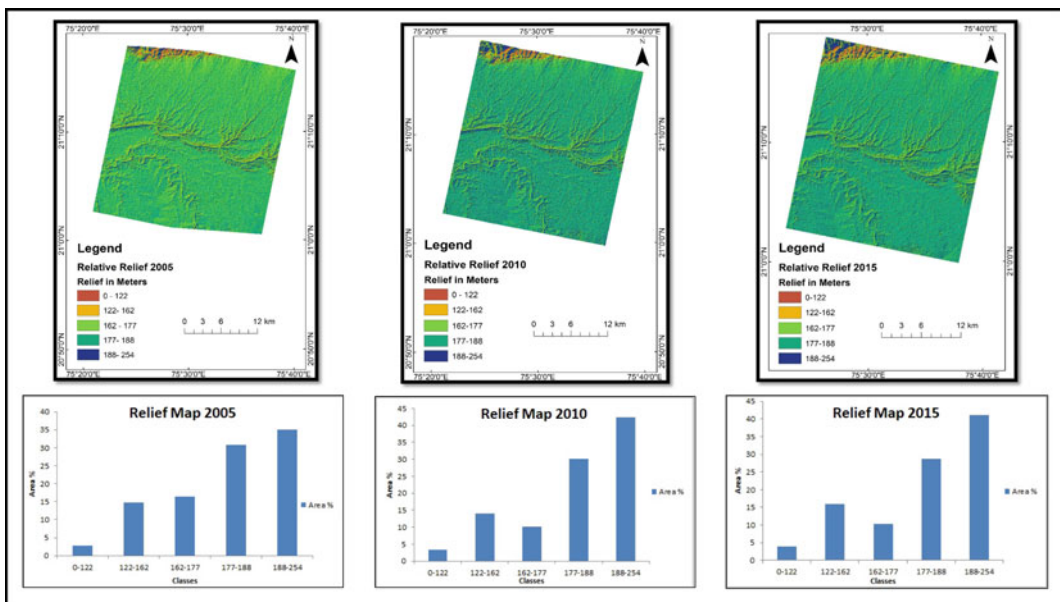
10.4.2.4 Exchangeable of Sodium Percentage (ESP)

The presence of excessive amount of exchangeable sodium reverses the process of aggregation
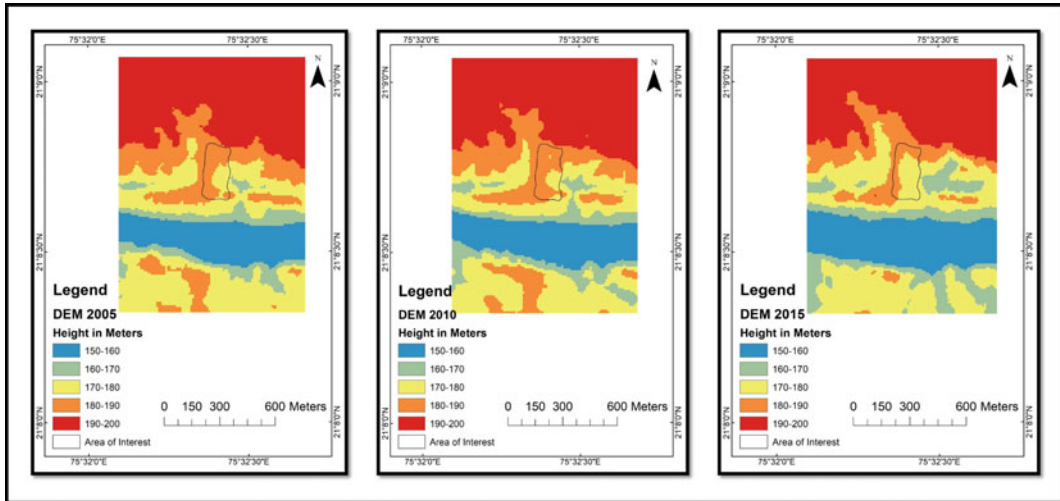
Fig. 10.6 DEMs of 2005, 2010 and 2015, with 10 m resolution

Fig. 10.7 Relief maps and their categories, for the three time periods (2005, 2010 and 2015)

and causes soil aggregates to disperse into their constituent individual soil particle. The sodic soil with few stabilizing agents in topsoil will ultimately succumb to erosion during heavy rain spells via rill or gully erosion. This is especially the case in soil with high silt and clay particle size fractions. Soil sodicity leads to decreased permeability and poor soil drainage over time. The soil with 6% or more content of ESP is known as sodic soil. This is an important parameter because sediments higher than 15% ESP are susceptible to slacking and piping.

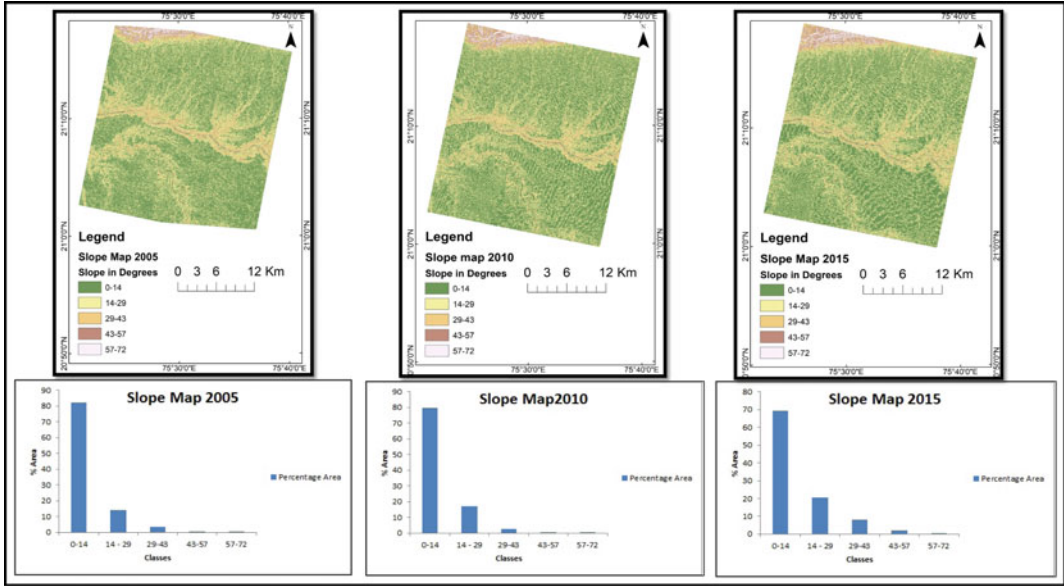The formula used for calculating ESP is as follows;

Fig. 10.8 Slope maps and their categories, for the three time periods (2005, 2010 and 2015)
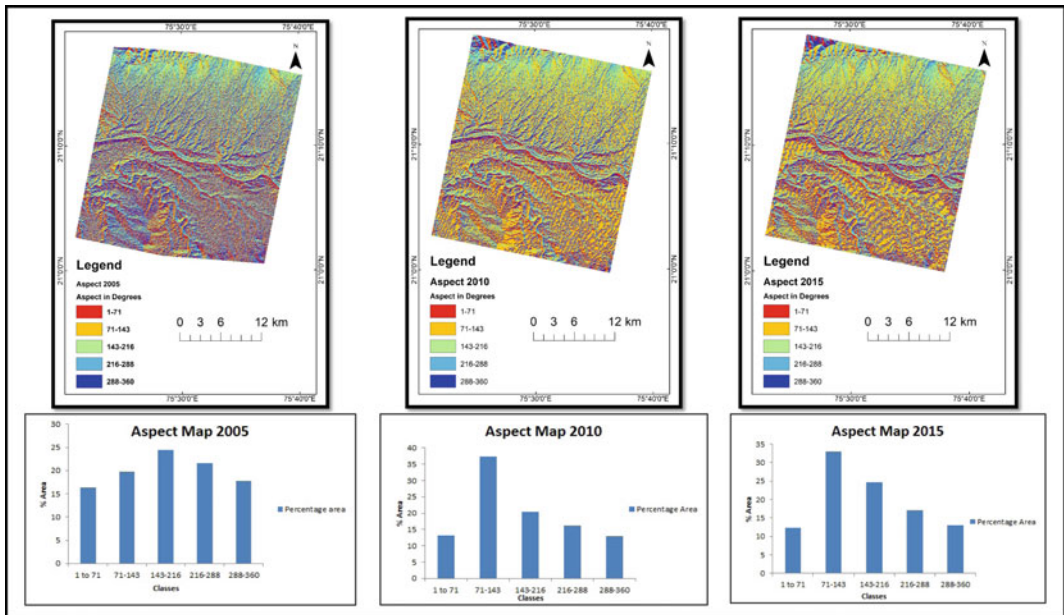

Fig. 10.9 Aspect maps and their categories, for the three time periods (2005, 2010 and 2015)

$$ESP = Exchangeable \ \{(Na)/(Ca + Mg + K + Na)\} * 100$$
$$(10.1)$$

Most of the samples ESP range in the value between 5 and 15% (Fig. 10.12). The average

value is 10.33%. The high values of ESP indicate that the soils on an average are fairly sodic which measures the erodibility of soil. Some of the detected samples are non-sodic in nature. But on an average, maximum samples fall in the
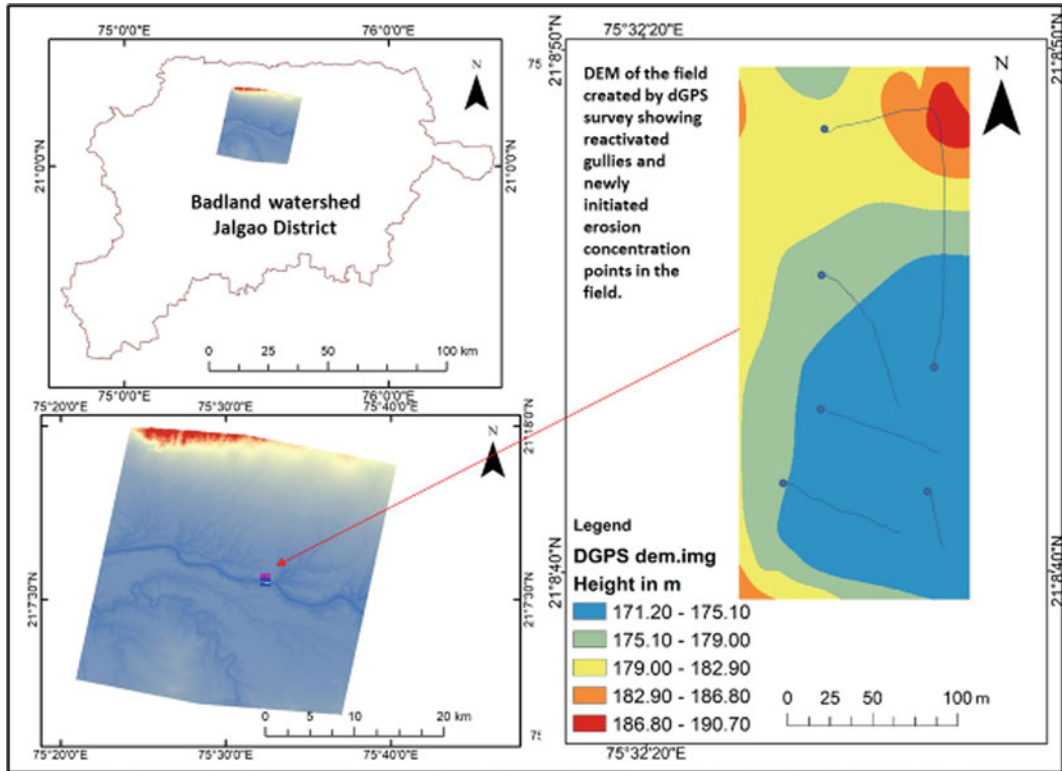
Fig. 10.10 DEM of the field under review created by field survey using dGPS with resolution of 5 cm. Many erosion concentration points can be seen on the DEM, which are following the original gully network

category of moderately sodic class. An association of pH with the general sodicity of the sediments has been depicted in Fig. 10.11 that indicates that samples having pH value between 8 and 10 are sodic in nature. ESP values for the samples indicate that they can be put under the category of moderate to highly erodible category. The pH of 25 samples from the area shows the value between 7 and 9, that also supports the observation.

10.4.2.5   Granulometric Parameter

Textural analysis of the fifteen samples was carried out by using sieving for the coarse sands and sedigraph for silt and clay. It is evident from Fig. 10.12 that silt content is higher than sand and clay in all the samples. Sand allows water to transmit through and hence soil containing higher percentage of sand is not erodible. Clay has the property of forming compact layer as well

as shrink and well under wet and dry conditions. They also have strong colloid binding and hence they also do not fall under the category of erodible soils. When soils contain higher percentage of silts, they are known to be highly susceptible to water erosion.

10.4.2.6   *K* Value (Erodibility of Soil)

Some soils have the tendency to erode more than others. This is due to the inherent properties of the soil and not due to any external factor. This is termed as soil erodibility. Soil texture is an important factor whilst studying erodibility. Gravels which require more force to transport are difficult to erode. On the contrary clay particles which are finer are also stable due to their cohesiveness. The most mobile and transportable particles are the very fine sand and silt particles. Organic matter has a big influence on the aggregate stability of the soils. Soils less than
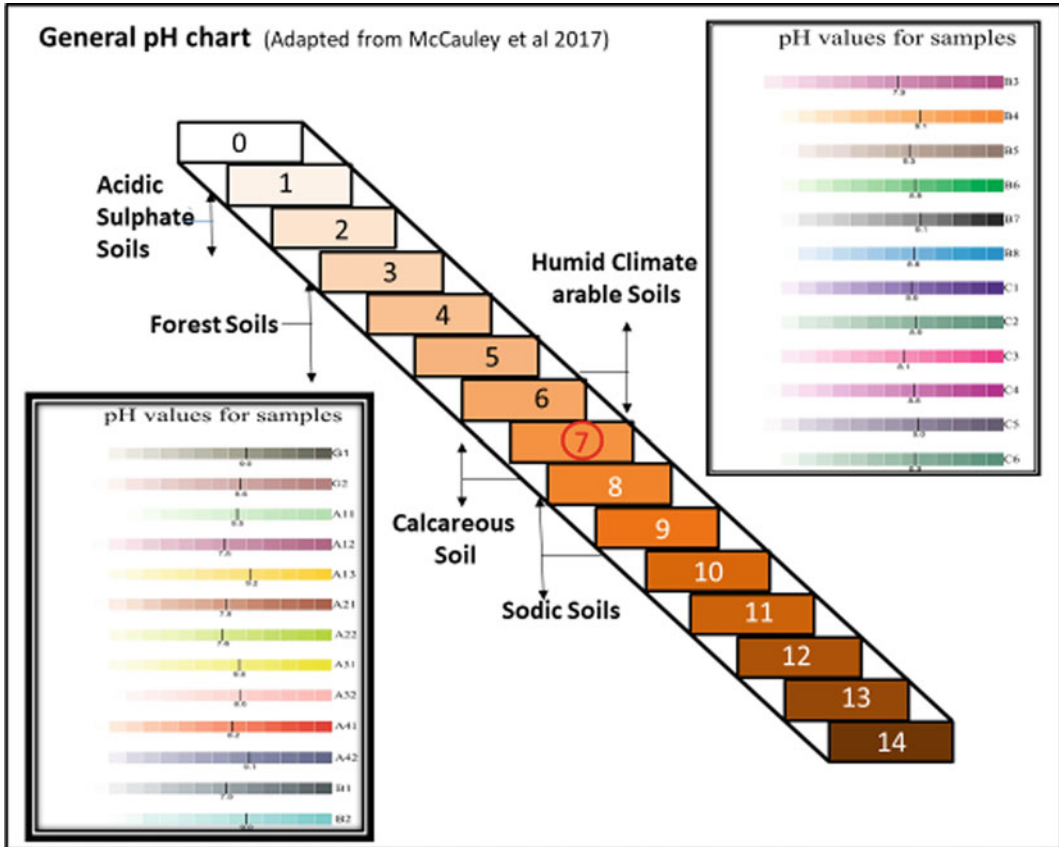
Fig. 10.11 General pH chart in the center (adapted from McCauley et al. 2017) and the pH of the samples from the field. The diagram shows the relation between pH and sodicity of the sediments

3.5% of organic matter are considered erodible. Moreover, clay particles combine with organic matter to form soil aggregates or clods which are usually resistant to erosion. K factor (erodibility) is lessened by larger structural aggregates and rapid soil permeability. However, the erodibility of a soil is the function of complex interactions between the various physical, chemical as well as mineralogical properties of soil. (Morgan 1986). The formula for calculating the K value employed in the study is given below;

$$k = 2.1 \times 10^{-6} * f_p^{1.14}(12 - P_{om}) + 0.0325(S_{stru} - 2) + 0.025(f_{pem} - 3)$$

$$(10.2)$$

where,

f_p $P_{silt}*(100-P_{clay})$
P_{om} Percent organic matter
S_{stru} Soil structure code used in soil classification
f_{pem} Profile permeability class.

Fifteen samples were selected for calculating the erodibility "K" index. Silt textural group (very fine sand + Silt) forms maximum part of the soils of this region. Numerical codes were assigned to both permeability and soil structure. The soil structure was estimated from field observation and the permeability was detected by testing the soil in Zuare Agro Pvt. Ltd., Pune. The average K value is 0.24, ranging between
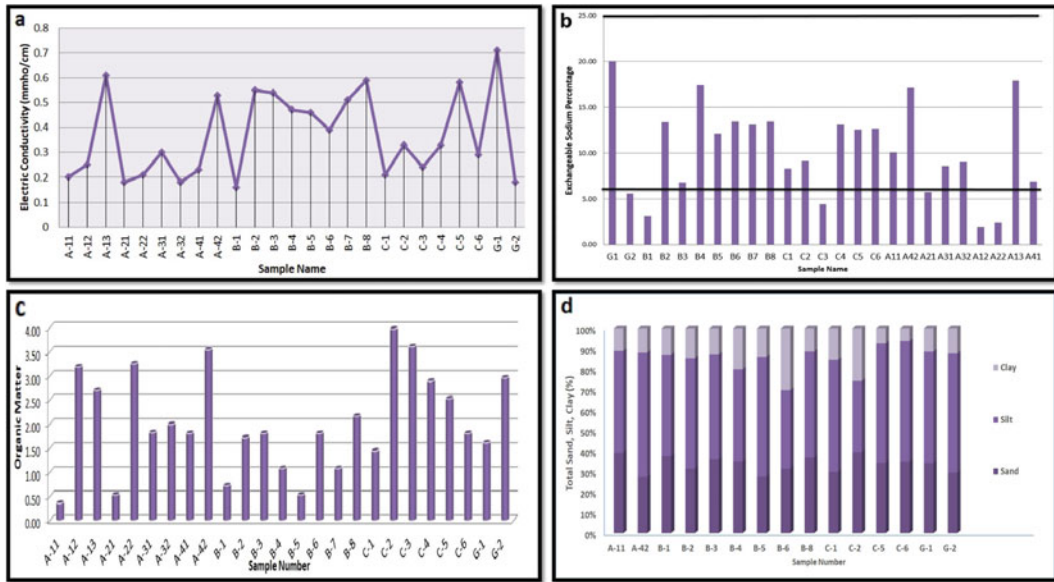
Fig. 10.12 The diagram depicts the results of four sediment parameters of the area (**a** electric conductivity, **b** exchangeable sodium percentage, **c** percentage organic matter, **d** sediment textural classes

Table 10.1 Soil erodibility (K Index) for the samples

Sample No.	K value	Sample No.	K value
1	0.29	9	0.28
2	0.29	10	0.13
3	0.27	11	0.35
4	0.30	12	0.34
5	0.25	13	0.29
6	0.23	14	0.26
7	0.34	15	0.30
8	0.25		

0.325 and 0.162. Erodibility as indicated by this index is not very high (Table 10.1).

10.4.2.7 Mean Scour Depth

Lacey-Inglis's method of estimating regime depth of flow in loose bed alluvial rivers was first developed by Lacey in 1929 and later by Inglis in 1944 mainly based on the observations of canals in India and neighbouring Pakistan. This technique is therefore used mainly in India for estimation of scour depth around bridge piers in alluvial channels. This technique has been applied in the present study to estimate the susceptibility of the alluvial topsoil forming the

badlands. The mean scour depth below the highest flood level (HFL) for natural channels flowing over scourable bed can be calculated theoretically from the following equation,

$$d_{sm} = 1.34 \left(D_b^2 / K_{sf} \right)^{1/3} \quad (10.3)$$

(Source: Indian Road Congress, IRC—5,1998).

Where,

d_{sm} Mean depth of scour in m below the highest flood level

D_b Discharge in cumecs per m width

K_{sf} Silt factor determined for the stratum based on weighted mean diameter of particle in mm.

The silt factors of the samples and estimated scour depth for various silt factors have been displayed in Table 10.2 and the estimated design scour depths for the samples results are outlined in Table 10.3. The mean scour depths of the sediments range in value between 3.06 and 4.39 m. In other words, if the sediments would have been under water, the top 4 m is the portion most vulnerable to erosion under the set of conditions prevailing in the area. These sediments are bank sediments and are directly in contact with water most time of the year, therefore assuming a situation close to the scouring conditions is applicable here.

The calculations are based on $D_b = 1.0$ cumecs per meter width and severe bend is considered.

10.4.3 Rainfall Factor (R)

Rainfall plays the most crucial parameter whilst studying erosion. Erosion index is a measure of the erosivity or erosive force of a specific rainfall event (Wischmeier and Smith 1965). The rainfall factor "R" of USLE is the number of erosion-index units in a normal year's rain. Wischmeier and Smith (1978) proposed that "R" factor must include the combined effects of moderate, as well as, severe storms on soil loss. The erosivity of rain in other words is the potential ability of rain to cause erosion. It is controlled by the physical characteristics of the rain. Babu et al. (1978) had developed the relationship between average annual erosion index (R factor) and annual rainfall, as well as, seasonal (June–September) rainfall for India based on their analysis of data from 44 stations spread across various rainfall zones of the country. The relationship is thus expressed as;

Table 10.2 Silt factor for different grades of soil and estimated scour depth for various silt factor

Type of bed material	Silt factor	Scour depth (m)	Design scour depth (m)
Fine silt	0.5	2.51	4.39
Silt	0.6	2.37	4.15
Medium sand	1.25	1.86	3.26
Coarse sand	1.5	1.75	3.06

Source (Indian Road Congress) IRC—5 1998

Table 10.3 Scour depth of the samples

Sample No.	Silt factor	Mean scour depth below HFL(m) as per IRC:78	Mean scour depth below HFL (m) assuming $D_b^* = 4.2$ Cumecs/m
1	0.35	$1.90 \times Db^{0.67}$	4.97
2	0.55	$1.64 \times Db^{0.67}$	4.28
3	2.59	$0.98 \times Db^{0.67}$	2.55
4	2.20	$1.03 \times Db^{0.67}$	2.69
5	0.35	$1.9 \times Db^{0.67}$	4.97
6	0.55	$1.64 \times Db^{0.67}$	4.28
7	0.55	$1.64 \times Db^{0.67}$	4.28
8	0.55	$1.64 \times Db^{0.67}$	4.28
9	2.59	$0.98 \times Db^{0.67}$	2.57
10	0.35	$1.64 \times Db^{0.67}$	4.97
11	0.35	$1.64 \times Db^{0.67}$	4.97
12	0.55	$1.64 \times Db^{0.67}$	4.28

D_b^* Design discharge for foundation per metre with effective linear waterway

$$R = 79 + 0.363P, \quad r = 0.83 \qquad (10.4)$$

where,

R   Average annual erosion index i.e. R in
    metric units
P   Average annual rainfall in mm.

In the present study, the equation (Eq. 10.4) has been used to compute R (rainfall erosivity) factor. Daily rainfall data (in mm) for the 15-year period from 1998 to 2012 for 15 meteorological stations of Jalgaon District (obtained from the Indian Meteorological Department, Pune) was used to compute the R factor. From the daily rainfall data, the average annual rainfall in Jalgaon was found to be 708.72 mm and the R factor was calculated to be 336.26.

10.4.3.1   Estimated Return Period of the Rainfall

Return period of 60-year rainfall has been calculated for the rainfall of the study area from 1955 to 2015. The highest rainfall during this period was 119.6 mm on 9th Sep. 1960, with a return period of 50 years. Second highest was in 1957 with an amount of 108.7 mm on 22-Jun-1957. Based on these data, estimated return period of 500 years have been calculated employing eight statistical techniques. The techniques used and their parameters have been demonstrated in Fig. 10.13. Out of the eight techniques used for trial estimate, the most suitable three techniques were finally chosen using Anderson–Darling goodness-of-fit test statistic (Table 10.4).

The Anderson–Darling statistic measures how well the data follows a particular distribution. For a given data set and distribution, the better the distribution fits the data, the smaller this statistic will be. Based on this result, the first three ranking techniques, such as, Lognormal (3P), Weibull (3P) and Log-Pearson 3 have been chosen and the final estimates have been made and produced in Fig. 10.13 and Table 10.5. It is interpreted that according to Lognormal (3P) estimate, a rain event of 171 mm/day may occur once in 100 years in these areas, 155 mm/day according to Weibull (3P)'s estimate and

142 mm/day after Log-Pearson 3. The five-hundred-year estimate goes up to 227 mm/day.

The data presented above implies that the chances of a rain event of 227 mm/day occurring in this region are once in 500 years or an event of 194 mm/day is 200 years. If it happens, it will create catastrophe in these fields and everything will get eliminated. Effect will be even more pronounced when the land is disturbed and loosened by the cultivation of crops. Figure 10.2 clearly showed that when undisturbed, these badland slopes are stabilized by vegetation reducing vulnerability. The real threat is when the watershed is disturbed, that progresses towards positive feedback of the system.

10.4.4   Morphometric Parameters

10.4.4.1   Stream Length (SL INDEX) Ratio

For a long time, geomorphology has made use of morphological analysis for the study of evolution and interpretation of landforms. Empirical methods were the major sources for the understanding of morphogenetic processes. From the Carto DEM of 2015, eight badland watersheds have been demarcated as shown in Fig. 10.14. Twenty-four profiles (approximately 3 profiles from each watershed) were drawn from the top of the badland surface to the main river. The semi-log graphs of these badland gullies are presented in Fig. 10.15a, b. All the graphs reveal above-grade condition, indicating a high energy topography and high competence of the badland streams/gullies. The distance between the gullies and the main river is short, hence this also will enhance the rapidity in erosion.

Several physical and mathematical methods were envisaged and applied by many researchers, mainly after 1950 to evaluate the energy of stream network and one amongst such methods one was put forward by Hack (1973) known as Stream Length-Gradient Index (SL Index). This was to determine whether a river would be in geomorphological equilibrium based upon the relationship between the river slope and the areal extent of the watershed.
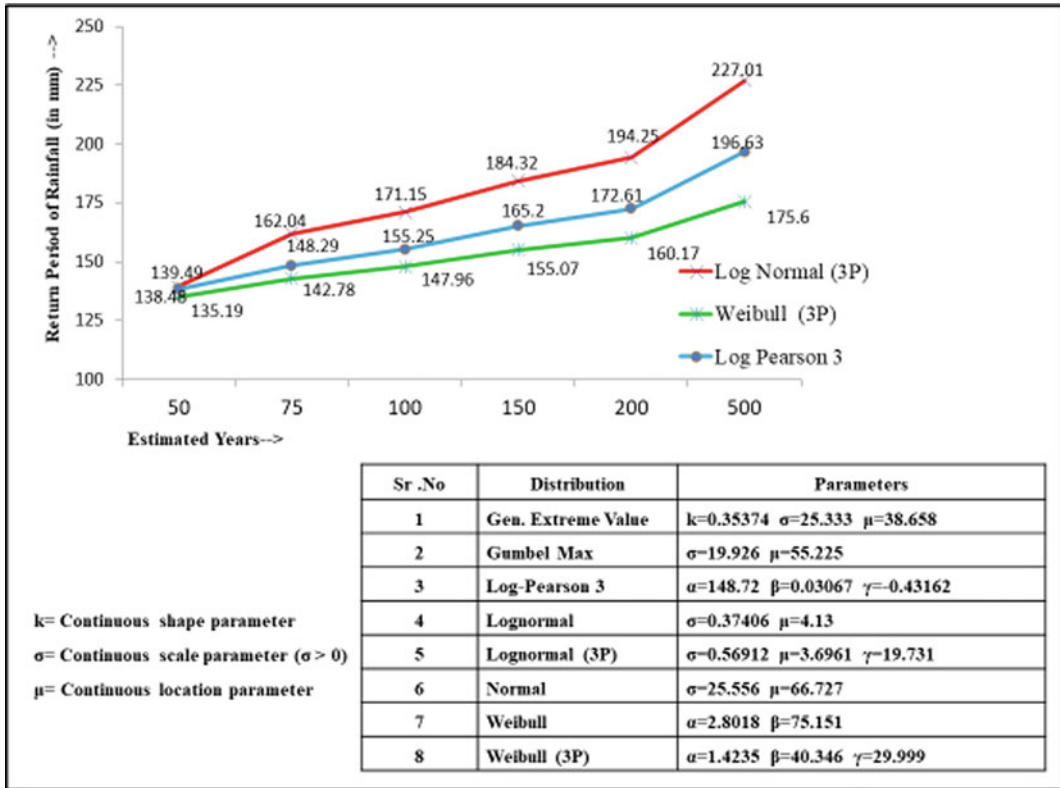
Fig. 10.13 Estimated return period of the rainfall for 500 years, for the three top ranking techniques, such as, Lognormal (3P), Weibull (3P) and Log Pearson 3 (based on Anderson–Darling goodness-of-fit test). Inset is the parameters of the eight statistical techniques used for the trial statistics in Anderson–Darling goodness-of-fit test

Table 10.4 Anderson–Darling goodness-of-fit test

Sr.No	Distribution	Anderson–Darling	
		Statistic	Rank
1	Lognormal (3P)	3.6375	1
2	Weibull (3P)	3.658	2
3	Log-Pearson 3	4.2103	3
4	Lognormal	4.4388	4
5	Gumbel Max	4.7363	5
6	Gen. extreme value	4.7465	6
7	Weibull	5.488	7
8	Normal	6.2589	8

$$\mathrm{SL} = h_1 - h_2 / \ln L_2 - \ln L_1 \qquad (10.5)$$

where

1. SL is Hack's Stream Gradient Index.
2. h_1 is the height of first point.
3. h_2 is the height of second point.
4. L_1 is the distance from source to first point.
5. L_2 is the distance from source to second point.

**Table 10.5** Estimated return period of rainfall for 500 years

Return period (year)	Probability %	Lognormal (3P) (daily rainfall in mm)	Weibull (3P) (daily rainfall in mm)	Log Pearson 3 (daily rainfall in mm)
50	0.98	139.49	135.19	138.48
75	0.9867	162.04	142.78	148.29
100	0.99	171.15	147.96	155.25
150	0.9933	184.32	155.07	165.2
200	0.995	194.25	160.17	172.61
500	0.998	227.01	175.6	196.63
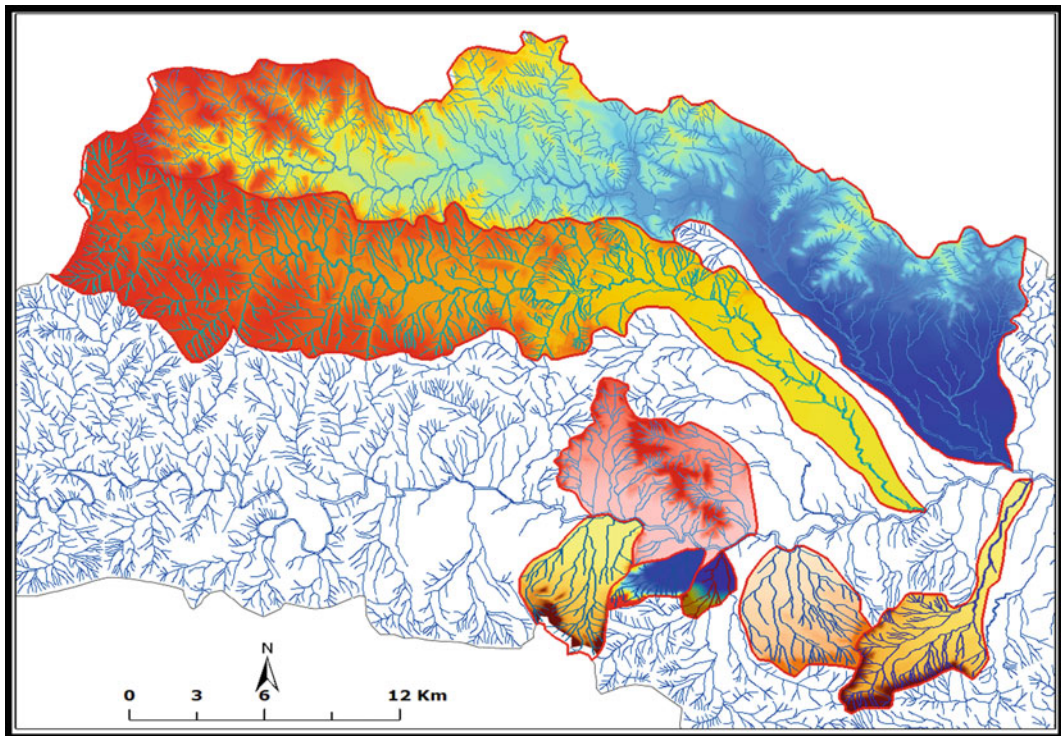
Fig. 10.14 Eight small gully watersheds have been demarcated from 2015 DEM to construct longitudinal profiles and calculate SL Indices

The calculated average SL index value is 211.9072 and the range is between 185 and 240 (Table 10.6). All the profiles are well above the grade level and are actively eroding. Considering the dimensions of the landscape under review, the profile lengths are short and the falls are considerable, overall competence of the streams are high enough to cause rapid erosion in a disturbed watershed.

10.5   Discussion

The present study is a geomorphic evaluation of the feasibility of the present land use pattern to an actively eroding badland and deeply disturbed watershed in a part of the Deccan Trap Region in Maharashtra. Summary of all the indices is depicted in Table 10.7. Together with that,
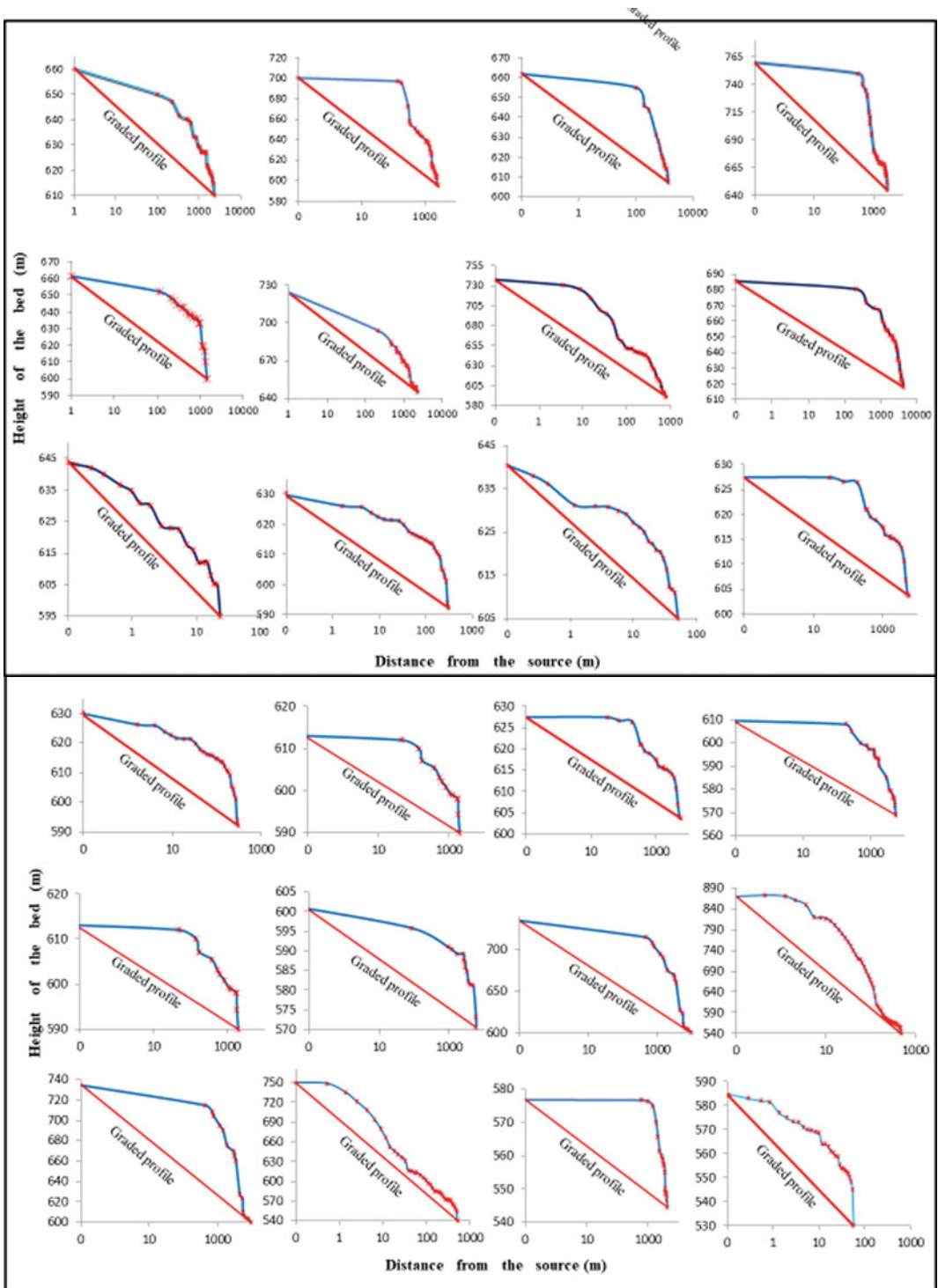
Fig. 10.15 Semi-log profiles of twentyfour badland gullies in the watershed. All the profiles show above-grade condition and high competence

Table 10.6 Hack's (1978) stream gradient index

Number	SL index	Number	SL index
1	240.4334	13	202.5267
2	202.5267	14	205.8139
3	206.629	15	215.8893
4	210.2172	16	216.0215
5	217.5934	17	216.6736
6	216.7907	18	184.6005
7	207.4577	19	220.1867
8	220.1867	20	196.9366
9	196.9366	21	185.6005
10	185.6005	22	212.0038
11	223.0071	23	218.2869
12	240.4334	24	213.3614

Google Earth images were also studied to see changes in the area.

Google Earth images and the DEMs along with the field photographs reveal that the AOI is undergoing a rapid change. There is a steady increase in the reclamation of badland areas and consequences of gully reactivation from 2005 till the present. The biggest change was observed in 2013 when some heavy spells destroyed the artificial wall across the gully and caused widespread gully erosion. Photographs taken from the field in 2013 provided a good evidence of the severity of gully erosion in the area. The gullies were finally filled in 2016 and brought under cultivation once again.

During the recent field visit to this area, reactivation of the gullies and the erosion concentration points were observed all over and also documented in the DEM generated from a field survey. Blocking the gullies and filling them offer just a temporary solution but the energy of the landscape is not diminished. Rainwater will flow with the same vigour and find its way to the river, eroding all the way. It is very clearly seen in the field that several minor rills and two major ones have already formed on the field. With time, it will deepen and once again the old network of gullies will be reactivated, unless a well-engineered diversion is created.

Sediment properties play a crucial role in understanding the erosion scenario of any watershed. Several sediment parameters were detected in the study that are relevant to the objective of the study. The current soil samples contain more percentage of silt and hence more susceptible to erosion. Sediment samples are sodic and calcareous in nature. Sodic soils are prone to a higher erosion rate. Carbon content of the average samples is less than 2%. considering this factor, we can say that soils in this area are not resistant to external force of raindrop impact or runoff. The physicochemical analysis of clay samples shows that if organic matter contents can be increased to values above 2%, then remodelled fields tend to stabilize. As a result, some badlands were being irreversibly destroyed and would be better classified as vanishing (Phillips 1998a, b). The values of electric conductivity are normal ranging from 0.16 to 0.71 mmho/cm. If the EC is low the rate of removal of soil is low and if the rate of removal is high the EC is higher.

When, Na concentrations are high enough to produce sodic soils, erodibility is maximized. Soils with lower electrolyte levels can disperse at lower ESP (Amezketa et al. 2003). Sodium forms a thick layer which will tend to move the clay/soil platelets farther apart and make them more susceptible to dissociation in any environment. The soil with 6% or more content of ESP is known as sodic soil. This is an important parameter because sediments higher than 15% ESP are susceptible to slacking and piping. Most of the samples tend

Table 10.7 Summary of the indices and the results

Parameters	Sub-parameters	Index values	Remarks/interpretations
Sediment	Textural	Silt 60–65%	Erodible
	OM	Avg 1.96%	Less than threshold value of 2 for stability
	ESP	10–15% in majority	Erodible for smectite rich soils
	EC	0.16–0.71 mmho/cm	Variable
	PH	Between 7 and 10	Towards Sodicity
	Silt factor and Scour depth	Between 2.55 m and 4.97 m	In other words, the top 4 m of the sediment is the portion most susceptible to erosion under the set of conditions prevailing in this area
	ESPdepth	Decreasing with dept	Uncertain
	K factor	Avg. 0.24 Between 0.325 and 0.162	Moderately erodible
	Clay	Hydroxy Interlayered Smectites	Shrink-swell, highly erodible (Joshi and Tambe 2008)
Morphometric	Slope Categories	Significantly altered from 2005–2015	Badland reclamation
	Slope aspect	Significantly altered from 2005–2015	
	Relative relief	Significantly altered from 2005–2015	
	Longitudinal profiles	SL Index 211.9 Avg - range between 185 and 240	Well above Grade High energy slopes
Rainfall	Erosivity	R = 336.26	Erosive, especially the first few storms of the monsoon when the badland slopes are bare
	Return period (500)	Lognormal (3P)— 227 mm/day Weibull (3P)— 175.6 mm/day Log-Pearson 3— 196.63 mm/day	Catastrophic Event
dGPS Field survey			Several evidence of reactivation of the earlier filled up gullies

towards sodicity in nature, indicating high erodibility. Overall erodibility based on "K" index show medium to fairly erodible nature of the sediments. Design scour depth of the sediments indicates the susceptibility of the top 4 m of these badland sediments. SL index of 24 samples reveal the above grade high energy system of these badland gullies and streams. Return periods of the high storm events in the region for 50–500 years reveal that 227 mm/day can occur once in 500 years. However stable as of the short term, nothing will stand against a rain event of this dimension in long term.

10.6 Conclusion

On the basis of the data generated during the course of this investigation which have been presented in the previous chapters and

summarized in the above paragraphs, it can be concluded that land use is changing very rapidly in this region. During the field visits, there were long interviews with the farmers of the area. Their input became very valuable during the study. First evidence of land filling was vague but it's on record that at least twice the field had been filled in the recent past after constructing an earthen wall across the main tributary gully. The wall breached twice after heavy monsoon rains and the gully network got activated both the times. The last breaching happened during 2013 monsoon. Last filling was performed in 2016 and the field was cultivated again. Around 1000 truckload of soil were dumped to fill these gullies. A rough calculation yielded around 7000 tons of soil that was used to fill these gullies, which is equal to 7000 tons of sediment being eroded from a single field in one monsoon event (qualitative assessment). The same situation is prevailing everywhere within the basin.

Compilation of the entire data generated during the study suggests that the region under review has already crossed the threshold of the tolerance limit of soil erosion mainly as the result of human activities. Though badlands are dynamic landscape, they are stable if they are not disturbed. It is when the natural landscape processes are completely altered by rapid actions of human, that a new set of processes start to develop in such areas to cope with the newly imposed systems. That is what we see in this area. The energy of the system is controlled by the relief and triggered by an erodible soil. Each time, the system goes back to positive feedback mechanism.

From the above discussion it can be concluded that levelling the terrain after clearing the vegetation and filling the natural gullies for farming etc. will not provide a future of agriculture in the area. A soft and hard engineering plan is necessary to divert the channel flow energy. Badlands are complex landscapes and it is not easy to plan diversion channels. Researches need to be conducted that focus on to suggest a more sustainable way of reclamation than

what is being practiced now. Sometimes successful operation of badland stabilization has been reported after treating the soil to reduce the threshold of erosion (Phillips 1998a, b), such as, the *calanche* and *biancane* badlands of Italy and Tuscany. This was possible by treating the sodicity of the soil, bringing the ESP below 15% threshold value. Such disappeared badlands are classified as "Vanishing Landscape" in the Red List of Mediterranean landscapes. However, the present study area will never be a vanishing landscape by treating the sediments. A hard/soft engineering design is recommended.

Finally, it is inferred that the area under review, like many other parts of the country is developing rapidly in agriculture. The arable fertile plains are already exhausted hence the further expansion of the activity is by exploiting the badlands, which were once considered unproductive. The only issue that should be seriously considered is whether this development (at the expense of the natural geomorphic feature) is going to be beneficial in the long run or otherwise. By levelling and smoothening the slopes, the natural processes that have long been operating in the area will not suddenly change. The method used by the farmers has already shown degradation in the land. The long-term benefit of the entire activity looks bleak. A land use planning needs to be designed for the gully infested areas because the present crude methods will lead more soil erosion than what was already experiencing in the area.

References

Abdel-Kader F (2018) Assessment and monitoring of land degradation in the northwest coast region, Egypt using Earth observations data. Egypt J Remote Sens Space Sci. https://doi.org/10.1016/j.ejrs.2018.02.001

Ajayi A (2015) Land degradation and the sustainability of agricultural production in Nigeria: A review. J Soil Sci Environ Manag 6:234–240

Amezketa E, Aragues R, Carranza R, Urgel B et al (2003) Chemical, spontaneous and mechanical dispersion of clays in arid-zone soils. Span J Agric Res 1:95–107

Babu R, Tejwani KG, Agarwal MP, Bhushan LS et al (1978) Distribution of erosion index and iso-erosion map of India. Indian J Soil Conserv 6(1):1–12

Bajocco S, Angelis AD, Perini L, Ferrara A, Salvati L et al (2012) The impact of land use/land cover changes on land degradation dynamics: a Mediterranean case study. Envron Manag 49:980–989

Batunacun WR, Lakes T, Yunfeng H, Nendel C et al (2019) Identifying drivers of land degradation in Xilingol, China, between 1975 and 2015. Land Use Pol 83:543–559

Bryan RB, Jones JA (1997) The significance of soil piping processes: inventory and prospect. Geomorphology 20:209–218

Canton Y, Barrio GD, Sole-Benet A, Lazaro R et al (2004) Topographic controls on the spatial distribution of ground cover in the Tabernas badlands of SE Spain. CATENA 22:341–365

Cowie AL, Orr BJ, Castillo Sanchez VM, Chasek P, Crossman ND, Erlewein A, Louwagie G, Maron M, Metternicht GI, Minelli S et al (2018) Land in balance: the scientific conceptual framework for land degradation neutrality. Environ Sci Policy 79:25–35

Dong A, Chesters G, Simsiman GV et al (1983) Soil dispersibility. Soil Sci 136(4):208–212

Gallart F, Mariganani M, Perez-Gallego N, Santi E, Maccherini S et al (2012) Thirty years of studies on badlands, from physical to vegetational approaches. A succinct review. CATENA. https://doi.org/10.1016/j.catena.2012.02.008

Gupta RK, Bhumbla DK Abrol IP et al (1984) Effect of sodicity, pH, organic matter and calcium carbonate on the dispersion behaviour of soils. Soil Sci 137(4):245–251

Hack JT (1973): Stream-profile analysis and stream-gradient index: U.S. Geological Survey. Journal Research, 1(4): 421–429

Hualin X, Yanwei Z, Zhilong W, Tiangui L et al (2020) A Bibliometric analysis on land degradation: current status, development, and future directions, Land 9:28. https://doi.org/10.3390/land9010028

Hazbavi Z, Sadeghi SHR, Gholamalifard M et al (2019) Dynamic analysis of soil erosion-based watershed health. Geogr Environ Sustain 3:43–59

Inglis CC (1944) Maxium depth of scour at heads of guide banks, groyens, pier noses and downstream of bridges. Annual Report (Technical), CWPRS, Pune

IRC (1998) Standard specifications and code practice for rod bridges section 1. IRC 5:1998

Joshi VU, Nagare V (2009) Land use and land cover change detection along the Pravara river basin in Maharashtra, using remote sensing and GIS techniques. Acta Geodaetica ET Geophysica Hungarica, AGD Lands Environ 3(2):71–86

Joshi VU, Tambe D (2008) Formation of Hydroxy - Interlayer Smectites (HIS) as an evidence for paleoclimatic changes along the riverine sediments of Pravara River and its tributaries in Maharashtra. Clay Res 27(1–2):1–12

Khaledian Y, Kiani F, Ebrahimi S, Brevik E, Aitkenhead-Peterson J et al (2016) Assessment and monitoring of soil degradation during land use change using multivariate analysis. Land Degrad Dev 28:128–141

Lacey G (1929) Stable channels in alluvium. J Inst Eng 4736:229

Lal R (1993) Tillage effects on soil degradation, soil resilience, soil quality, and sustainability. Soil Tillage Res. 27:1–8

Marathianou M, Kosmas C, Gerontidis S, Detsis V et al (2000) Land-use evolution and degradation in Lesvos (Greece): a historical approach. Land Deg Dev 11(1):63–73

Matano AS, Kanangire CK, Anyona DN, Abuom PO, Gelder FB, Dida GO, Owuor PO, Ofulla AVO et al (2015) Effects of land use change on land degradation reflected by soil properties along Mara River, Kenya and Tanzania. Open J Soil Sci 5:20–38

McCauley A, Jones C, Olson-Rutz K (2017) Soil pH and organic matter. Nutrient management. Module no 8. 1–12

Mongil-Manso J, Navarro-Hevia V, Díaz-Gutiérrez V, Cruz-AlonsoI V, Ramos-Díez I et al (2016) Badlands forest restoration in Central Spain after 50 years under a Mediterranean-continental climate. Ecol Eng 97:313–326

Morgan RPC (1986) Soil erosion and conservation. Longman Group Ltd., Essex

Muneer M, Oades JM (1989) The role of Ca–organic interactions in soil aggregate stability. III. Mechanisms and models. Aust J Soil Res 27:411–423

Phillips C (1998a) a) The badlands of Italy: a vanishing landscape? Appl Geogr 18(3):243–257

Phillips C (1998b) The Crete Senesi, Tuscany: a vanishing landscape? Landsc Urban Plan 41(1):19–26

Piegay H, Walling DE, London N, He Q, Liebault F, Petiot R et al (2004) Contemporary changes in sediment yield in an alpine mountain basin due to afforestation (the upper Drome in France). CATENA 55(2):183–212

Reynolds JF, Stafford SM (eds) (2002) Global desertification: Do humans cause deserts? Dahlem University Press, Berlin

Rossi R, Vos W (1993) Criteria for the identification of a red list of Mediterranean landscapes: three examples in Tuscany. Landsc Urban Plan 24:233–239

Saha AK, Arora MK, Csaplovies E, Gupta RP et al (2005) Land cover classification using IRS LISS III image

and DEM in Rugged Terrain; a case study in Himalayas. Geocarto Int 20(2):33–40

Sangsub C, Chan-Beom K, Jeonghwan K, Ah Lim L, Pa K-H, Namin K, Yong SK et al (2020) Land-use changes and practical application of the land degradation neutrality (LDN) indicators: a case study in the subalpine forest ecosystems. Republic Korea Forest Sci Technol 16(1):8–17

Wischmeier WH, Smith DD (1965) Rainfall-erosion losses from cropland east of the rocky mountains: guide for selection of practices for soil and water conservation. USDA Agriculture Research Series, Agriculture Handbook No. 282

Wischmeier WH and Smith DD (1978) Predicting rainfall erosion losses: A guide to conservation planning, USDA Agr. Res. Ser., Agriculture Handbook No. 537.

Wells NA, Andreamiheja B (1993) The initiation and growth of gullies, Madagascar-Are humans to be blamed? Geomorphology 8:1–46

Zhang K, Yu Z, Li X, Zhou W, Zhang D et al (2007) Land use change and land degradation in China from 1991 to 2001. Land Degrad Dev 18:209–219